

Sterile Neutrinos and Supernova Nucleosynthesis

David O. Caldwell¹, George M. Fuller², and Yong-Zhong Qian^{3*}

¹*Institute for Nuclear and Particle Astrophysics and Cosmology, and Department of Physics,
University of California, Santa Barbara, CA 93106*

²*Department of Physics, University of California, San Diego, La Jolla, CA 92093-0319*

³*School of Physics and Astronomy, University of Minnesota, Minneapolis, MN 55455*

(August 8, 2021)

Abstract

A light sterile neutrino species has been introduced to explain simultaneously the solar and atmospheric neutrino puzzles and the results of the LSND experiment, while providing for a hot component of dark matter. Employing this scheme of neutrino masses and mixings, we show how matter-enhanced active-sterile ($\nu_{\mu,\tau} \rightleftharpoons \nu_s$) neutrino transformation followed by active-active ($\nu_{\mu,\tau} \rightleftharpoons \nu_e$) neutrino transformation can solve robustly the neutron deficit problem encountered by models of r -process nucleosynthesis associated with neutrino-heated supernova ejecta.

PACS number(s): 14.60.Pq, 14.60.St, 26.30.+k, 97.60.Bw

Typeset using REVTeX

*On leave from T-5, MS B283, Los Alamos National Laboratory, Los Alamos, NM 87545.

I. INTRODUCTION

In this paper we show how the invocation of sterile neutrinos in a novel transformation scenario can enable the production of the heavy rapid-neutron-capture (r -process [1]) elements in neutrino-heated ejecta from supernovae. Interestingly, the current hints of (and constraints on) neutrino oscillation phenomena from considerations of solar [2] and atmospheric neutrinos [3] and from the LSND experiment [4] are difficult to explain with only two independent neutrino mass-squared differences (corresponding to three active neutrino species) [5]. By contrast, the data are explained readily in terms of neutrino oscillations with three independent mass-squared differences, corresponding to four neutrino masses [6,7]. However, the observed width of the Z^0 [8] can accommodate only three light, active neutrinos. Therefore, a fit to the data requires introducing at least one light “sterile” neutrino species which does not have normal weak interactions [e.g., a Majorana SU(2) singlet neutrino].

The most promising site for r -process nucleosynthesis is the neutrino-heated material ejected relatively long (~ 10 s) after the explosion of a Type II or Type Ib/c supernova [9]. However, detailed calculations of the conditions which obtain above the neutron star remnant in such r -process models show that the neutron-to-seed ratio, R , is too low to allow the production of the heaviest r -process species [10]. (The “seed” nuclei which capture neutrons to make the heavier species have nuclear mass numbers between 50 and 100.) We require $R > 100$ to effect a good r -process yield for heavy nuclear species, but the models with conventional neutrino physics and conventional equations of state for nuclear matter all give smaller values of R . This is the neutron deficit problem for these models of the r -process.

In all models, R is determined by the net electron-to-baryon number (i.e., the electron fraction), Y_e , the entropy-per-baryon in the ejecta, S , and the dynamic expansion timescale, τ_{DYN} , associated with the material ejection process [10]. Though general relativistic effects [11] and multi-dimensional hydrodynamic outflow [12] have been invoked to increase S and

decrease τ_{DYN} (both of these changes favoring larger R) enough to solve the neutron deficit problem, these solutions are at best finely tuned. On general grounds we could argue that the only robust way to obtain $R > 100$ in conventional *neutrino-heated* ejecta is to decrease Y_e and/or maintain its low value by invoking new neutrino physics, e.g., introducing a sterile neutrino as discussed in this paper. (By “robust” we mean robust to astrophysical uncertainties in the detailed characteristics of neutrino-heated outflow.) We cannot definitively proclaim at this point that new neutrino physics is required to understand the production of heavy r -process elements. Such a proclamation calls for the accomplishment of the following. First, we would have to establish that at least some of the r -process material originates in conventional neutrino-heated ejecta. Second, we would have to understand the thermal and hydrodynamic evolution of the very late stage neutrino-driven “winds” from a proto-neutron star.

The proposition that some of the r -process material comes from environments with intense neutrino fluxes is supported by recent studies of neutrino effects during and immediately following the r -process [13,14]. Perhaps more to the point, recent observational data on the abundances of r -process species in old, very metal-poor halo stars in the Galaxy seem to be quite consistent with what is expected from the r -process scenario associated with neutrino-heated ejecta [15]. However, the second issue we would have to resolve is a vexing one. Despite the extensive numerical insights into the early phase of the supernova evolution [16], consistent and accurate hydrodynamic scenarios for neutron stars to lose mass through neutrino heating at very late times remain to be established. On the positive side, Burrows [17] has recently followed his supernova calculations long enough to see the formation of a neutrino-driven wind at late times. In the region relevant for nucleosynthesis, the wind in his calculations resembles in broad brush the outflow models studied here.

This paper is organized as follows. In Sec. II, we describe a simple model for the neutrino-heated outflow and discuss the associated alpha effect which causes the neutron deficit problem for r -process nucleosynthesis. In Sec. III, we discuss the treatment of active-sterile plus active-active neutrino transformation in supernovae and describe how

such transformation can evade the alpha effect. The consequence of such transformation for the evolution of the electron fraction Y_e in the neutrino-heated outflow is studied in Sec. IV. Conclusions are given in Sec. V.

II. NEUTRINO-HEATED OUTFLOW AND THE ALPHA EFFECT

In what follows we adopt a simple exponential wind model for the neutrino-driven outflow above the surface of the hot proto-neutron star produced by a supernova explosion. In this model the enthalpy per baryon is roughly the gravitational binding energy of a baryon, leading to a relation between radius r_6 (in units of 10^6 cm), entropy-per-baryon S_{100} (in units of 100 times the Boltzmann constant), and temperature T_9 (in units of 10^9 K):

$$r_6 \approx \frac{22.5}{T_9 S_{100}} \left(\frac{M_{\text{NS}}}{1.4 M_{\odot}} \right), \quad (1)$$

where M_{NS} is the mass of the proto-neutron star. Therefore, for a constant entropy per baryon characterizing the adiabatic expansion of the outflow, the temperature parameterizes the radius [11]. The entropy typically will be carried almost exclusively by relativistic particles (photons and electron-positron pairs) so that $S \approx (2\pi^2/45)g_s T^3/(\rho N_A)$, where g_s is the statistical weight for relativistic particles and N_A is Avogadro's number. This leads to a simple relation between (matter) density ρ and radius:

$$\rho \approx 3.34 \times 10^3 \text{ g cm}^{-3} \left(\frac{g_s}{11/2} \right) T_9^3 S_{100}^{-1} \approx 3.8 \times 10^7 \text{ g cm}^{-3} \left(\frac{M_{\text{NS}}}{1.4 M_{\odot}} \right)^3 \left(\frac{g_s}{11/2} \right) S_{100}^{-4} r_6^{-3}, \quad (2)$$

where we have scaled g_s assuming its value at $T_9 \gtrsim 10$. As we will be mostly interested in processes occurring at $T_9 \gtrsim 10$, the dependence on g_s will be suppressed hereafter.

In the exponential wind the radius of an outflowing mass element is related to time t by $r = r_0 \exp[(t - t_0)/\tau_{\text{DYN}}]$. Here τ_{DYN} is an assumed constant material expansion timescale. This implies an outflow velocity proportional to radius, $v = r/\tau_{\text{DYN}}$, so that the neutrino-driven wind will remain roughly self similar for timescales on which the neutrino luminosities and energy spectra and the neutron star radius can be regarded as constant. Clearly, at

some point above the neutron star surface the exponential wind must go over to a linear expansion of the radius, i.e., a “coasting” outflow. Nevertheless, the exponential wind regime should encompass the region above the neutron star where most of the biggest obstacle to successful r -process nucleosynthesis, the alpha effect (see below), is operative [13].

In neutrino-heated ejecta, neutrino interactions with matter supply the requisite energy for ejection of nucleosynthesis products. The total amount of heating through these interactions determines S and τ_{DYN} in the ejecta. Most of this heating occurs close to the neutron star and S and τ_{DYN} are set at $T_9 \sim 20$. However, the dominant interactions for neutrino heating

$$\nu_e + n \rightarrow p + e^- \quad (3)$$

and

$$\bar{\nu}_e + p \rightarrow n + e^+ \quad (4)$$

have prolonged effects on the neutron-to-proton ratio ($n/p = 1/Y_e - 1$) in the ejecta. First of all, in the region where $T_9 \gtrsim 10$ and free nucleons are favored by nuclear statistical equilibrium (NSE), the competition between the processes in Eqs. (3) and (4) leads to $n/p \approx \lambda_{\bar{\nu}_e p} / \lambda_{\nu_e n} \sim (L_{\bar{\nu}_e} \langle E_{\bar{\nu}_e} \rangle) / (L_{\nu_e} \langle E_{\nu_e} \rangle)$. Here $\lambda_{\bar{\nu}_e p}$ and $\lambda_{\nu_e n}$ are the rates for the reactions in Eqs. (4) and (3), respectively, $L_{\bar{\nu}_e}$ and L_{ν_e} are the $\bar{\nu}_e$ and ν_e energy luminosities, respectively, and $\langle E_{\bar{\nu}_e} \rangle$ and $\langle E_{\nu_e} \rangle$ are the average energies characterizing the corresponding neutrino energy spectra. Absent neutrino oscillations (flavor/type mixings), we expect $\langle E_{\nu_\mu} \rangle \approx \langle E_{\bar{\nu}_\mu} \rangle \approx \langle E_{\nu_\tau} \rangle \approx \langle E_{\bar{\nu}_\tau} \rangle > \langle E_{\bar{\nu}_e} \rangle > \langle E_{\nu_e} \rangle$ and, hence, $n/p > 1$ ($Y_e < 0.5$, corresponding to neutron-rich ejecta) [18]. We note that the numerical value of the n/p ratio depends on careful calculation of the rates $\lambda_{\bar{\nu}_e p}$ and $\lambda_{\nu_e n}$ [19] and accurate determination of $L_{\bar{\nu}_e}$, L_{ν_e} , $\langle E_{\bar{\nu}_e} \rangle$, and $\langle E_{\nu_e} \rangle$ [20]. However, the alpha effect discussed below is insensitive to the value of the n/p ratio obtained at $T_9 \gtrsim 10$.

The equilibrium of the n/p ratio with the ν_e and $\bar{\nu}_e$ fluxes described above is maintained until the ejecta passes the weak freeze-out radius (at $T_9 \sim 10$), r_{WFO} , beyond which $\lambda_{\nu_e n}$,

$\lambda_{\bar{\nu}_e p} < 1/\tau_{\text{DYN}}$ and free nucleons are no longer favored by NSE [18]. However, even beyond r_{WFO} , ν_e capture on neutrons can force down the n/p ratio and, hence, the neutron-to-seed ratio R . This is the so-called ‘‘alpha effect’’ [21,13]: as material flows to regions where the composition favored by NSE shifts from free nucleons to a mixture of free nucleons and alpha particles, protons will be incorporated into alpha particles, leaving a disproportionate fraction of neutrons exposed to the intense flux of ν_e . The process in Eq. (3) then converts some of these neutrons into protons (which are then immediately incorporated into alpha particles), thus progressively lowering the n/p ratio and, ultimately, R .

The cumulative damage done to the n/p ratio by ν_e capture on neutrons beyond the weak freeze-out radius r_{WFO} can be estimated crudely by integrating $dY_e/dt \approx \lambda_{\nu_e n}(t)(1 - 2Y_e)$ to obtain

$$Y_e(t) \approx 0.5 + [Y_e(0) - 0.5] \exp \{-\lambda_{\nu_e n}(0)\tau_{\text{DYN}}[1 - \exp(-2t/\tau_{\text{DYN}})]\}, \quad (5)$$

where initial values for the ν_e capture rate on neutrons and the electron fraction, $\lambda_{\nu_e n}(0)$ and $Y_e(0)$, respectively, can be approximated as their values at r_{WFO} . Equilibrium of the n/p ratio with the ν_e and $\bar{\nu}_e$ neutrino fluxes at early times requires that $\lambda_{\nu_e n}(0)\tau_{\text{DYN}} \sim 1$. Furthermore, the product $\lambda_{\nu_e n}(0)\tau_{\text{DYN}}$ should be roughly constant for all models with conventional neutrino physics, since increased (decreased) neutrino luminosity will tend to increase (decrease) $\lambda_{\nu_e n}$ and decrease (increase) τ_{DYN} proportionately. [Neutrino heating through the processes in Eqs. (3) and (4), which set Y_e , is the principal determinant of τ_{DYN} .] Therefore, from Eq. (5) it can be seen that regardless of the freeze-out value $Y_e(0)$, sufficient exposure to the ν_e flux above r_{WFO} will drive Y_e close to 0.5 ($n/p = 1$, i.e., no neutron excess).

In summary, a great paradox exists for r -process nucleosynthesis in a neutrino-driven wind. In such a scenario the neutrinos must supply enough energy [largely through the processes in Eqs. (3) and (4)] to lift baryons out of the gravitational potential well of the neutron star. The gravitational binding energy per nucleon near the neutron star surface is ~ 100 MeV. Since the average ν_e and $\bar{\nu}_e$ energies are ~ 10 MeV, a nucleon must interact with neutrinos ~ 10 times in order to acquire enough energy for ejection from the neutron

star. In turn, this requires a sufficiently large value of $\lambda_{\nu_e n}(0)\tau_{\text{DYN}}$, thus providing conditions for a pernicious alpha effect which will cause a neutron deficit. Such a neutron deficit will preclude a successful r -process, especially the synthesis of the heaviest nuclear species.

However, it is obvious that removal of the ν_e flux could neatly solve the neutron deficit problem by unbalancing the competition between the processes in Eqs. (3) and (4) in favor of neutron production (thus lowering Y_e) and by disabling the alpha effect in regions beyond r_{WFO} (thus maintaining a low Y_e). Furthermore, as neutrino heating is essentially completed at $T_9 \sim 20$ (quite close to the neutron star surface), the beneficial effects of removing the ν_e flux can be obtained without affecting the general thermal and hydrodynamic characteristics of the neutrino-heated outflow (see Sec. III).

III. EVASION OF THE ALPHA EFFECT VIA ACTIVE-STERILE PLUS ACTIVE-ACTIVE NEUTRINO TRANSFORMATION

The existence of at least one light sterile neutrino could provide a means to reduce the ν_e flux at sufficiently large radius to leave the process of neutrino-heated ejection unhindered, yet sufficiently near or inside r_{WFO} so as to disable the alpha effect, and thereby fix the neutron deficit problem for r -process nucleosynthesis. This r -process solution can be obtained by having an active-sterile ($\nu_{\mu,\tau} \rightleftharpoons \nu_s$) neutrino mass-level crossing followed by an active-active ($\nu_{\mu,\tau} \rightleftharpoons \nu_e$) neutrino mass-level crossing. (Hereafter, ν_s and $\bar{\nu}_s$ denote left- and right-handed Majorana sterile neutrinos, respectively.) The first mass-level crossing converts ν_μ and ν_τ , which are emitted with the highest average energy from the neutron star, into harmless sterile neutrinos. Without this, significant conversion of ν_μ and ν_τ into ν_e would drive the neutrino-heated supernova ejecta proton rich [18]. With the supernova ν_μ and ν_τ “sterilized” by the first mass-level crossing, the second mass-level crossing now only acts to convert ν_e emitted from the neutron star into ν_μ and ν_τ . Charged-current capture reactions on neutrons are energetically forbidden for supernova ν_μ and ν_τ . The net result is that the ν_e flux is reduced or removed, and the alpha effect cannot operate. Therefore, the neutron

excess is preserved or possibly enhanced in this scenario.

The sequence of neutrino mass-level crossings described above can occur in a four-neutrino scheme [6] which has two nearly degenerate neutrino doublets separated by a mass-squared difference chosen to be compatible with the LSND $\nu_\mu \rightleftharpoons \nu_e$ signal. In this scheme the lower mass neutrino pair would either give an active-sterile $\nu_e \rightleftharpoons \nu_s$ mass-level crossing in the sun, or provide a “just so” vacuum mixing solution with $\delta m_{es}^2 \sim 10^{-10} \text{ eV}^2$ to the solar neutrino problem [22]. For solving the solar neutrino problem via matter-enhanced $\nu_e \rightleftharpoons \nu_s$ mixing, the mass-squared splitting for the lower mass neutrino pair must be $\delta m_{es}^2 \lesssim 10^{-5} \text{ eV}^2$ [22]. The mass-squared splitting for the higher mass neutrino pair is chosen to explain the observed atmospheric ν_μ/ν_e data via maximal $\nu_\mu \rightleftharpoons \nu_\tau$ vacuum mixing.

Figure 1 shows our adopted neutrino mass scheme. The mass-squared splittings shown are chosen to meet all experimental constraints and to solve the neutron deficit problem for r -process nucleosynthesis associated with neutrino-heated supernova ejecta. We would require $m_{\nu_s} > m_{\nu_e}$ for matter-enhanced $\nu_e \rightleftharpoons \nu_s$ mixing in the sun, but a “just so” solution to the solar neutrino problem could have $m_{\nu_s} < m_{\nu_e}$ as well. (Issues of compatibility with Big Bang Nucleosynthesis limits aside, note that some kinds of singlet “sterile neutrinos” could possibly evade bounds on the “just so” $\nu_e \rightleftharpoons \nu_s$ vacuum mixing solution stemming from the SuperK and the Chlorine Experiments [23].) In our overall mass scheme ν_μ and ν_τ could share the role of providing a hot dark matter component [24].

Of the possible four-neutrino mass patterns, this one is most successful in evading constraints. It has been shown that limits from accelerator and reactor experiments disfavor having one dominant neutrino mass, e.g., a 3 + 1 or a 1 + 3 arrangement [25]. A two-doublet scheme with $\nu_\mu \rightleftharpoons \nu_s$ mixing (the higher mass pair) explaining the atmospheric neutrino anomaly and $\nu_e \rightleftharpoons \nu_\tau$ mixing (the lower mass pair) explaining the solar neutrino puzzle is in trouble with Big Bang Nucleosynthesis bounds [26].

With an appropriate choice of mixing angles and mass-squared difference for the splitting of the doublets, the neutrino mass scheme in Fig. 1 will lead to an efficient matter-enhanced $\nu_{\mu,\tau} \rightleftharpoons \nu_s$ transition above the neutron star surface (and the neutrino sphere), yet below

the region where an ordinary Mikheyev-Smirnov-Wolfenstein (MSW) [27] matter-enhanced $\nu_{\mu,\tau} \rightleftharpoons \nu_e$ mass-level crossing would occur [28]. Furthermore, the mass-level crossing for ν_e with energies most relevant for determining Y_e can still lie in the region near or below the weak freeze-out radius r_{WFO} .

A. General Description of Neutrino Flavor/Type Evolution in Supernovae

As discussed in Sec. IIIB, the overall problem of active-sterile plus active-active neutrino transformation in our case can be treated as that of two separate mass-level crossings, with each mass-level crossing involving effectively only two neutrino flavors/types. The neutrino flavor/type evolution through each mass-level crossing is governed by a Schroedinger-like equation:

$$i \frac{d}{dt} \begin{bmatrix} a_x(t) \\ a_y(t) \end{bmatrix} = (H_v + H_e + H_{\nu\nu}) \begin{bmatrix} a_x(t) \\ a_y(t) \end{bmatrix}, \quad (6)$$

where $a_x(t)$ and $a_y(t)$ are the time-dependent amplitudes for the neutrino to be in, for example, the flavor eigenstates $|\nu_e\rangle$ and $|\nu_\mu\rangle$, respectively. The propagation Hamiltonian in Eq. (6) is given as the sum of three terms H_v , H_e , and $H_{\nu\nu}$ resulting from vacuum masses, forward scattering on electrons and nucleons, and forward scattering on “background” neutrinos, respectively.

In general, we can express the neutrino propagation Hamiltonian as:

$$H_v + H_e + H_{\nu\nu} = \frac{1}{2} \begin{pmatrix} -\Delta \cos 2\theta + A + B & \Delta \sin 2\theta + B_{\text{off}} \\ \Delta \sin 2\theta + B_{\text{off}}^* & \Delta \cos 2\theta - A - B \end{pmatrix}, \quad (7)$$

where $\Delta \equiv \delta m^2/(2E_\nu)$, with E_ν the neutrino energy and δm^2 the appropriate vacuum neutrino mass-squared difference, A is the appropriate electron/nucleon background contribution, and B and B_{off} are the diagonal and off-diagonal contributions, respectively, from the neutrino background. (The terms B_{off} and B_{off}^* are complex conjugates of each other and vanish in the case of active-sterile neutrino transformation.) Note that a mass-level crossing or resonance will occur if the following condition is satisfied:

$$\Delta \cos 2\theta = A + B. \quad (8)$$

Table I gives appropriate expressions for the weak potentials A and B for all possible cases of 2×2 active-sterile and active-active neutrino mixings in terms of density ρ (in g cm^{-3}), Avogadro's number N_A , Y_e , and the effective neutrino numbers for each of the three active species relative to baryons, Y_{ν_e} , Y_{ν_μ} , Y_{ν_τ} .

The effective neutrino number for species α ($\alpha = e, \mu, \tau$) relative to baryons is $Y_{\nu_\alpha} = (n_{\nu_\alpha}^{\text{eff}} - n_{\bar{\nu}_\alpha}^{\text{eff}})/\rho N_A$, where for example, the effective number density of neutrino species α at position r encountered by a “test” neutrino traveling in a pencil of directions $\hat{\Omega}$ is [18,29,30],

$$n_{\nu_\alpha}^{\text{eff}} \approx \sum_{\beta} \frac{1}{c\pi R_\nu^2} \frac{L_{\nu\beta}}{\langle E_{\nu\beta} \rangle} \int_0^\infty dE_{\nu\beta} \int \frac{d\hat{\Omega}'}{4\pi} f_{\nu\beta}(E_{\nu\beta}) P_{\nu\beta \rightarrow \nu_\alpha}(E_{\nu\beta}, r, \hat{\Omega}') (1 - \hat{\Omega}' \cdot \hat{\Omega}). \quad (9)$$

Here β runs over all neutrino species to be considered (including species α), $f_{\nu\beta}(E_{\nu\beta})$ is the *normalized* energy distribution function for neutrino species β at its birth position (the neutrino sphere of radius R_ν), and $P_{\nu\beta \rightarrow \nu_\alpha}(E_{\nu\beta}, r, \hat{\Omega}')$ is the probability for an initial ν_β to appear as a ν_α when encountering the test neutrino at position r . In general, this transformation probability will depend on the energy $E_{\nu\beta}$ and direction $\hat{\Omega}'$ of the background neutrino ν_β , as well as on the position r . The last factor in Eq. (9) contains additional dependence on the direction $\hat{\Omega}'$ of the background neutrino.

For efficient conversion of neutrino flavors/types, evolution of the neutrino amplitudes through the mass-level crossing (resonance) must be adiabatic. In turn, this requires that the width of the resonance region be large compared with the local neutrino oscillation length. The width of the resonance region is

$$\delta r = \mathcal{H} \tan 2\theta, \quad (10)$$

where \mathcal{H} is the scale height of the weak potential at resonance:

$$\mathcal{H} \approx \left| \frac{d \ln(A + B)}{dr} \right|_{\text{res}}^{-1}. \quad (11)$$

The adiabaticity parameter γ characterizing the evolution of the neutrino amplitudes through resonance is proportional to the ratio of the resonance width to the local oscillation length:

$$\gamma = \frac{\delta m^2 \sin^2 2\theta}{2E_\nu \cos 2\theta} \mathcal{H} \approx 4.6 \left(\frac{\delta m^2}{6 \text{ eV}^2} \right) \left(\frac{25 \text{ MeV}}{E_\nu} \right) \left(\frac{\sin^2 2\theta}{10^{-3}} \right) \left(\frac{\mathcal{H}}{7.5 \text{ km}} \right). \quad (12)$$

Note that $\gamma > 3$ corresponds to better than 99% conversion of neutrino flavors/types.

B. The Case of Active-Sterile plus Active-Active Neutrino Transformation

In the context of the general scheme in Fig. 1 for neutrino masses and mixings we make several specifications to facilitate our goal of removing the bulk of the ν_e flux in the appropriate region above the neutrino sphere. First we invoke maximal mixing between ν_μ and ν_τ , which is consistent with the SuperK atmospheric neutrino data. Furthermore, we assume that the vacuum mixing between $\nu_{\mu,\tau}$ and $\nu_{e,s}$ is small. In particular, we consider the following mixing scheme between the flavor/type eigenstates and the vacuum mass eigenstates:

$$\begin{pmatrix} |\nu_e\rangle \\ |\nu_s\rangle \\ |\nu_\mu\rangle \\ |\nu_\tau\rangle \end{pmatrix} = \begin{pmatrix} \cos \phi & \sin \phi \cos \omega & \sin \phi \sin \omega & 0 \\ -\sin \phi & \cos \phi \cos \omega & \cos \phi \sin \omega & 0 \\ 0 & -\sin \omega / \sqrt{2} & \cos \omega / \sqrt{2} & 1 / \sqrt{2} \\ 0 & \sin \omega / \sqrt{2} & -\cos \omega / \sqrt{2} & 1 / \sqrt{2} \end{pmatrix} \begin{pmatrix} |\nu_1\rangle \\ |\nu_2\rangle \\ |\nu_3\rangle \\ |\nu_4\rangle \end{pmatrix}. \quad (13)$$

In Eq. (13), the vacuum mixing between ν_e and ν_s is largely governed by the angle ϕ , while that between ν_μ and ν_τ is chosen to be maximal by our assumption. The angle ω essentially specifies the vacuum mixing between $\nu_{\mu,\tau}$ and $\nu_{e,s}$. For small vacuum mixing between these two doublets, we require $\omega \ll 1$. In Eq. (13), all the CP-violating phases are ignored.

With the definition of

$$|\nu_\mu^*\rangle \equiv \frac{|\nu_\mu\rangle - |\nu_\tau\rangle}{\sqrt{2}}, \quad (14)$$

and

$$|\nu_\tau^*\rangle \equiv \frac{|\nu_\mu\rangle + |\nu_\tau\rangle}{\sqrt{2}}, \quad (15)$$

Eq. (13) can be rewritten as

$$\begin{pmatrix} |\nu_e\rangle \\ |\nu_s\rangle \\ |\nu_\mu^*\rangle \\ |\nu_\tau^*\rangle \end{pmatrix} = \begin{pmatrix} \cos\phi & \sin\phi\cos\omega & \sin\phi\sin\omega & 0 \\ -\sin\phi & \cos\phi\cos\omega & \cos\phi\sin\omega & 0 \\ 0 & -\sin\omega & \cos\omega & 0 \\ 0 & 0 & 0 & 1 \end{pmatrix} \begin{pmatrix} |\nu_1\rangle \\ |\nu_2\rangle \\ |\nu_3\rangle \\ |\nu_4\rangle \end{pmatrix}. \quad (16)$$

It is clear from Eq. (16) that $|\nu_\tau^*\rangle$ is a mass eigenstate in vacuum, i.e., $H_v|\nu_\tau^*\rangle \propto |\nu_\tau^*\rangle$. In fact, $|\nu_\tau^*\rangle$ is also an effective mass eigenstate in the presence of electron/nucleon and neutrino backgrounds, i.e., $(H_v + H_e + H_{\nu\nu})|\nu_\tau^*\rangle \propto |\nu_\tau^*\rangle$. This is because the amplitude of forward scattering on electrons and nucleons is the same for ν_μ and ν_τ while the effective number densities of ν_μ and ν_τ for neutrino-neutrino scattering above the neutrino sphere are the same due to the symmetry in transformations concerning ν_μ and ν_τ . Therefore, the evolution of $|\nu_\tau^*\rangle$ is decoupled from that of $|\nu_s\rangle$, $|\nu_e\rangle$, and $|\nu_\mu^*\rangle$.

As discussed above, maximal mixing between ν_μ and ν_τ allows us to reduce the problem of 4×4 neutrino mixing into that of mixing among ν_s , ν_e , and ν_μ^* . In the region above, yet not too far away from the neutrino sphere, this 3×3 neutrino mixing problem is characterized by the mass-level crossings for $\nu_\mu^* \rightleftharpoons \nu_s$ and $\nu_\mu^* \rightleftharpoons \nu_e$ transformations. Note that although $\delta m_{\mu^*s}^2 \approx \delta m_{\mu^*e}^2$ in our neutrino mass scheme shown in Fig. 1, the weak potentials A and B in the neutrino propagation Hamiltonian are quite different for $\nu_\mu^* \rightleftharpoons \nu_s$ and $\nu_\mu^* \rightleftharpoons \nu_e$ transformations. The effect of the weak potential B from the neutrino background will be addressed in Sec. IV. For simplicity, we will neglect B in the following discussion. According to Eq. (8) and Table I, the mass-level crossing (resonance) for $\nu_\mu^* \rightleftharpoons \nu_s$ transformation occurs when

$$\frac{\delta m_{\mu^*s}^2}{2E_\nu} \cos 2\theta_{\mu^*s} = \sqrt{2}G_F\rho N_A \frac{1 - Y_e}{2}, \quad (17)$$

while that for $\nu_\mu^* \rightleftharpoons \nu_e$ transformation occurs when

$$\frac{\delta m_{\mu^*e}^2}{2E_\nu} \cos 2\theta_{\mu^*e} = \sqrt{2}G_F\rho N_A Y_e. \quad (18)$$

In Eqs. (17) and (18), G_F is the Fermi constant, and θ_{μ^*s} and θ_{μ^*e} are the appropriate two-neutrino vacuum mixing angles. From Eq. (16) we have $\theta_{\mu^*s} \sim \omega \cos\phi \ll 1$ and $\theta_{\mu^*e} \sim \omega \sin\phi \ll 1$.

In our proposed scheme to enable the r -process in neutrino-heated supernova ejecta by disabling the alpha effect, we require that the $\nu_\mu^* \rightleftharpoons \nu_s$ conversion of relatively high energy neutrinos take place well below the weak freeze-out radius. The temperature at which weak freeze-out in the ejecta occurs is $T_9^{\text{WFO}} \approx 10$. According to Eqs. (2) and (17), conversion below (at smaller radii than) the weak freeze-out radius then requires

$$\delta m_{\mu^*s}^2 \gtrsim 3.8 \text{ eV}^2 \left(\frac{T_9^{\text{WFO}}}{10} \right)^3 \left(\frac{E_\nu}{25 \text{ MeV}} \right) \left[\frac{(1 - Y_e)/2}{0.3} \right] S_{100}^{-1}, \quad (19)$$

where we have taken $g_s = 11/2$, consistent with the conditions in the ejecta for $T_9 \gtrsim T_9^{\text{WFO}}$, and scaled the result assuming a typical value of $Y_e = 0.4$ as obtained in numerical supernova models in the absence of neutrino transformation. Similarly, for the $\nu_\mu^* \rightleftharpoons \nu_e$ resonance to occur below the weak freeze-out radius, we require

$$\delta m_{\mu^*e}^2 \gtrsim 5.1 \text{ eV}^2 \left(\frac{T_9^{\text{WFO}}}{10} \right)^3 \left(\frac{E_\nu}{25 \text{ MeV}} \right) \left(\frac{Y_e}{0.4} \right) S_{100}^{-1}. \quad (20)$$

Therefore, a value of $\delta m_{\mu^*s}^2 \approx \delta m_{\mu^*e}^2 \approx 6 \text{ eV}^2$ consistent with the LSND data would fulfill the requirements in Eqs. (19) and (20).

We note that for $Y_e > 1/3$, the $\nu_\mu^* \rightleftharpoons \nu_s$ resonance will occur before (at higher density and temperature than) the $\nu_\mu^* \rightleftharpoons \nu_e$ resonance for a given neutrino energy [cf. Eqs. (17) and (18)]. Specifically, the temperature at resonance is

$$T_{9,\mu^*s} \approx 11.6 \left(\frac{\delta m_{\mu^*s}^2}{6 \text{ eV}^2} \right)^{1/3} \left(\frac{25 \text{ MeV}}{E_\nu} \right)^{1/3} \left[\frac{0.3}{(1 - Y_e)/2} \right]^{1/3} S_{100}^{1/3} \quad (21)$$

for the $\nu_\mu^* \rightleftharpoons \nu_s$ case, and

$$T_{9,\mu^*e} \approx 10.6 \left(\frac{\delta m_{\mu^*e}^2}{6 \text{ eV}^2} \right)^{1/3} \left(\frac{25 \text{ MeV}}{E_\nu} \right)^{1/3} \left(\frac{0.4}{Y_e} \right)^{1/3} S_{100}^{1/3} \quad (22)$$

for the $\nu_\mu^* \rightleftharpoons \nu_e$ case. According to Eq. (1), the radial separation between the two resonances has a typical value of 2 km. As shown below, this is much larger than the widths of both resonance regions.

The scale height of the weak potential for both $\nu_\mu^* \rightleftharpoons \nu_s$ and $\nu_\mu^* \rightleftharpoons \nu_e$ resonances can be approximated as

$$\mathcal{H} \approx \left| \frac{d \ln \rho}{dr} \right|_{\text{res}}^{-1} \approx \frac{r_{\text{res}}}{3}, \quad (23)$$

where r_{res} is the radius for the relevant resonance, and we have neglected the change in Y_e compared with that in ρ . To ensure adiabatic conversion and accommodate the LSND data at the same time, we require $\sin^2 2\theta \sim 10^{-3}$ for $\theta = \theta_{\mu^*s}, \theta_{\mu^*e}$. [This is easily achieved by having $\omega \sim 10^{-2}$ and $\phi \sim \pi/4$ in Eq. (13).] From Eq. (10), the widths of the $\nu_\mu^* \rightleftharpoons \nu_s$ and $\nu_\mu^* \rightleftharpoons \nu_e$ resonance regions are $(\delta r)_{\mu^*s} \sim (\delta r)_{\mu^*e} \sim 0.2$ km, much smaller than the separation between the two resonances. Therefore, we can treat the evolution of ν_e as unaffected by the $\nu_\mu^* \rightleftharpoons \nu_s$ resonance and that of ν_s unaffected by the $\nu_\mu^* \rightleftharpoons \nu_e$ resonance.

So far we have restricted our discussion to the case of $Y_e > 1/3$. As the electron fraction Y_e gets close to $1/3$, the $\nu_\mu^* \rightleftharpoons \nu_s$ and $\nu_\mu^* \rightleftharpoons \nu_e$ resonances will approach each other and overlap. In addition, the weak potential governing the evolution of neutrino amplitudes will be dominated by the neutrino background for $Y_e \approx 1/3$. However, as discussed in Sec. IV, the transformation of neutrino flavors/types, coupled with the expected rapid expansion of the neutrino-heated ejecta, will cause the actual value of Y_e at a radius to differ significantly from the equilibrium value corresponding to the local ν_e and $\bar{\nu}_e$ fluxes. For interesting ranges of $\delta m_{\mu^*s}^2$ and $\delta m_{\mu^*e}^2$, the problematic neutrino evolution near $Y_e = 1/3$ occurs well beyond the weak freeze-out radius and does not affect our treatment of the $\nu_\mu^* \rightleftharpoons \nu_s$ and $\nu_\mu^* \rightleftharpoons \nu_e$ transformations discussed previously.

We have also ignored the possibility of a $\nu_e \rightleftharpoons \nu_s$ resonance in the treatment of active-sterile neutrino transformation. This is because were this resonance to occur below the weak freeze-out radius, neutrino evolution through this resonance would be grossly non-adiabatic for the neutrino mass-squared difference ($\delta m_{e_s}^2 \lesssim 10^{-5} \text{ eV}^2$) adopted to solve the solar neutrino problem in our neutrino mixing scheme [see Eq. (12)].

To summarize the discussion in this subsection, we depict the squares of the effective neutrino masses as functions of density in Fig. 2. Here we assume that $Y_e > 1/3$ and the order of the resonances is as shown. As Y_e decreases, the effective mass track for ν_μ^* will steepen, while that for ν_e will flatten out. For $Y_e < 1/3$ this trend will be so extreme that

the order of the resonances will reverse. As noted above and discussed in Sec. IV, for our adopted neutrino mixing parameters this reversal does not occur below the weak freeze-out radius in a typical neutrino-heated outflow.

C. Removal of the ν_e Flux and Evasion of the Alpha Effect

Based on the discussion in Sec. IIIB, we can regard the the $\nu_\mu^* \rightleftharpoons \nu_s$ and $\nu_\mu^* \rightleftharpoons \nu_e$ resonances as filters of neutrino flavors/types when neutrino evolution through these resonances is adiabatic. Consider the evolution of an initial neutrino state

$$|\nu(t = t_0)\rangle = a_e|\nu_e\rangle + a_s|\nu_s\rangle + a_{\mu^*}|\nu_\mu^*\rangle + a_{\tau^*}|\nu_\tau^*\rangle. \quad (24)$$

At $t > t_{\mu^*s}$, i.e., after adiabatic propagation through the $\nu_\mu^* \rightleftharpoons \nu_s$ resonance, the neutrino state becomes

$$|\nu(t > t_{\mu^*s})\rangle \approx a'_e|\nu_e\rangle + a'_s|\nu_\mu^*\rangle + a'_{\mu^*}|\nu_s\rangle + a'_{\tau^*}|\nu_\tau^*\rangle, \quad (25)$$

where the primed coefficients differ from the corresponding unprimed ones in Eq. (24) only by a phase. Symbolically, the function of the $\nu_\mu^* \rightleftharpoons \nu_s$ resonance can be described as $|\nu_e\rangle \rightarrow |\nu_e\rangle$, $|\nu_s\rangle \rightarrow |\nu_\mu^*\rangle$, $|\nu_\mu^*\rangle \rightarrow |\nu_s\rangle$, and $|\nu_\tau^*\rangle \rightarrow |\nu_\tau^*\rangle$. At $t > t_{\mu^*e} > t_{\mu^*s}$, i.e., after adiabatic propagation through the $\nu_\mu^* \rightleftharpoons \nu_e$ resonance, the neutrino state becomes

$$|\nu(t > t_{\mu^*e})\rangle \approx a''_e|\nu_\mu^*\rangle + a''_s|\nu_e\rangle + a''_{\mu^*}|\nu_s\rangle + a''_{\tau^*}|\nu_\tau^*\rangle, \quad (26)$$

where the double-primed coefficients differ from the corresponding unprimed ones in Eq. (24) again only by a phase. Symbolically, the function of the $\nu_\mu^* \rightleftharpoons \nu_e$ resonance can be described as $|\nu_e\rangle \rightarrow |\nu_\mu^*\rangle$, $|\nu_s\rangle \rightarrow |\nu_s\rangle$, $|\nu_\mu^*\rangle \rightarrow |\nu_e\rangle$, and $|\nu_\tau^*\rangle \rightarrow |\nu_\tau^*\rangle$.

The probabilities for the initial neutrino state in Eq. (24) to evolve into the $|\nu_e\rangle$, $|\nu_s\rangle$, $|\nu_\mu^*\rangle$, and $|\nu_\tau^*\rangle$ states after adiabatic propagation through the $\nu_\mu^* \rightleftharpoons \nu_s$ and $\nu_\mu^* \rightleftharpoons \nu_e$ resonances can be obtained from Eq. (26) as:

$$P_{\nu_e}(t > t_{\mu^*e}) \approx \left| \langle \nu_s | \nu(t = t_0) \rangle \right|^2, \quad (27)$$

$$P_{\nu_s}(t > t_{\mu^*e}) \approx \left| \langle \nu_\mu^* | \nu(t = t_0) \rangle \right|^2, \quad (28)$$

$$\begin{aligned} P_{\nu_\mu}(t > t_{\mu^*e}) &\approx \left| \langle \nu_\mu | \nu_\mu^* \rangle \langle \nu_e | \nu(t = t_0) \rangle + \langle \nu_\mu | \nu_\tau^* \rangle \langle \nu_\tau^* | \nu(t = t_0) \rangle \exp(i\Phi) \right|^2 \\ &\approx \frac{1}{2} \left(\left| \langle \nu_e | \nu(t = t_0) \rangle \right|^2 + \left| \langle \nu_\tau^* | \nu(t = t_0) \rangle \right|^2 \right), \end{aligned} \quad (29)$$

and

$$\begin{aligned} P_{\nu_\tau}(t > t_{\mu^*e}) &\approx \left| \langle \nu_\tau | \nu_\mu^* \rangle \langle \nu_e | \nu(t = t_0) \rangle + \langle \nu_\tau | \nu_\tau^* \rangle \langle \nu_\tau^* | \nu(t = t_0) \rangle \exp(i\Phi) \right|^2 \\ &\approx \frac{1}{2} \left(\left| \langle \nu_e | \nu(t = t_0) \rangle \right|^2 + \left| \langle \nu_\tau^* | \nu(t = t_0) \rangle \right|^2 \right). \end{aligned} \quad (30)$$

In Eqs. (29) and (30) the second approximation is obtained by averaging over the phase Φ .

From Eqs. (27)–(30) we see that after adiabatic evolution through the $\nu_\mu^* \rightleftharpoons \nu_s$ and $\nu_\mu^* \rightleftharpoons \nu_e$ resonances, (1) a ν_e emitted from the neutron star [i.e., $|\nu(t = t_0)\rangle = |\nu_e\rangle$] would become 50% ν_μ and 50% ν_τ ; (2) a ν_μ emitted from the neutron star [i.e., $|\nu(t = t_0)\rangle = |\nu_\mu\rangle$] would become 50% ν_s , 25% ν_μ , and 25% ν_τ ; and (3) a ν_τ emitted from the neutron star [i.e., $|\nu(t = t_0)\rangle = |\nu_\tau\rangle$] would become 50% ν_s , 25% ν_μ , and 25% ν_τ . Clearly, as no sterile neutrinos are emitted from the neutron star, the ν_e flux would be removed at those energies for which adiabatic evolution through the $\nu_\mu^* \rightleftharpoons \nu_s$ and $\nu_\mu^* \rightleftharpoons \nu_e$ resonances is completed. Therefore, if such neutrino evolution can be engineered to occur below the weak freeze-out radius and convert most of the ν_e emitted from the neutron star to other species before the electron fraction falls near or below 1/3, then we will have succeeded in disabling the alpha effect.

IV. THE EVOLUTION OF THE ELECTRON FRACTION WITH ACTIVE-STERILE PLUS ACTIVE-ACTIVE NEUTRINO TRANSFORMATION

Consider the Y_e evolution of a mass/fluid element moving outward from the neutron star surface (i.e., the neutrino sphere). In the absence of neutrino flavor/type transformation,

this fluid element would be irradiated by the ν_e , $\bar{\nu}_e$, ν_μ , $\bar{\nu}_\mu$, ν_τ , and $\bar{\nu}_\tau$ fluxes emitted from the neutrino sphere throughout its progress toward ejection. (There should not be an *appreciable* flux of sterile neutrinos coming from the neutron star interior. Though a small sterile neutrino flux will not affect our conclusions, it is nonetheless interesting to note that for our assumed scheme of neutrino masses and mixings, matter effects inside the proto-neutron star should suppress strongly the production of sterile neutrinos.) Of course, the occurrence of the $\nu_\mu^* \rightleftharpoons \nu_e$ resonance will cause the fluid element to experience deviation of its Y_e evolution from the standard case with no neutrino flavor/type transformation.

As discussed in Sec. IIIB, the $\nu_\mu^* \rightleftharpoons \nu_s$ resonance occurs before (at higher temperature than) the $\nu_\mu^* \rightleftharpoons \nu_e$ resonance for $Y_e > 1/3$. Further, neutrinos with lower energies generally go through the two resonances before those with higher energies. Consequently, the two resonances will sweep through the relevant neutrino energy distribution functions when viewed in the frame of a fluid element as it moves from the neutrino sphere at high temperature towards regions of lower temperature. The energy-position of the $\nu_\mu^* \rightleftharpoons \nu_e$ resonance within the distribution functions, i.e., the resonance energy E_ν^{RES} , is related to temperature T_9 and radius r_6 through the resonance condition as

$$\begin{aligned} E_\nu^{\text{RES}} &\approx 29.4 \text{ MeV} \left(\frac{\delta m_{\mu^*e}^2}{6 \text{ eV}^2} \right) \left[\frac{0.4}{Y_e + Y_{\nu_e} - (Y_{\nu_\mu} + Y_{\nu_\tau})/2} \right] \left(\frac{10}{T_9} \right)^3 S_{100} \\ &\approx 2.58 \text{ MeV} \left(\frac{\delta m_{\mu^*e}^2}{6 \text{ eV}^2} \right) \left[\frac{0.4}{Y_e + Y_{\nu_e} - (Y_{\nu_\mu} + Y_{\nu_\tau})/2} \right] \left(\frac{1.4 M_\odot}{M_{\text{NS}}} \right)^3 S_{100}^4 r_6^3. \end{aligned} \quad (31)$$

When a fluid element reaches a given radius, we can regard all ν_e emitted from the neutrino sphere with energies less than the corresponding E_ν^{RES} at this radius as having changed to either ν_μ or ν_τ . Note that no conversion into ν_e occurs as the $|\nu_\mu^*\rangle$ component of the ν_μ or ν_τ emitted from the neutrino sphere with the relevant energies will have been converted into sterile neutrinos before reaching the $\nu_\mu^* \rightleftharpoons \nu_e$ resonance. (Adiabatic neutrino evolution through the $\nu_\mu^* \rightleftharpoons \nu_s$ and $\nu_\mu^* \rightleftharpoons \nu_e$ resonances is assumed here.) The ν_e and $\bar{\nu}_e$ capture rates in the fluid element, $\lambda_{\nu_e n}$ and $\lambda_{\bar{\nu}_e p}$, respectively, will both decrease with increasing radius due to the geometric dilution of the neutrino fluxes. However, as E_ν^{RES}

increases, conversion into ν_μ or ν_τ will further decrease the ν_e flux in addition to the geometric dilution. Consequently, the rate $\lambda_{\nu_{en}}$ for raising Y_e will decrease more with increasing radius than the rate $\lambda_{\bar{\nu}_{ep}}$ for lowering Y_e . One would then expect Y_e to be lowered progressively as the fluid element moves towards larger radius. If $Y_e \lesssim 1/3$ is reached, the order of the $\nu_\mu^* \rightleftharpoons \nu_s$ and $\nu_\mu^* \rightleftharpoons \nu_e$ resonances will reverse (see Sec. IIIB) and further transformation of ν_e will cease. In principle this could be worrisome as the evasion of the alpha effect requires that the bulk of the ν_e flux over a substantial range of energies be transformed away prior to the point of alpha-particle formation.

However, in practice the defeat of the alpha effect through removal of the ν_e flux will be achieved for the expected conditions in the neutrino-heated ejecta and plausible neutrino mixing parameters. This is because ν_e conversion coupled with the expected rapid expansion of the ejecta will cause the actual value of Y_e at a given radius to differ significantly from the equilibrium value corresponding to the local ν_e and $\bar{\nu}_e$ fluxes. This equilibrium value at radius r is defined as

$$Y_e^{\text{EQ}}(r) \equiv \frac{\lambda_{\nu_{en}}(r)}{\lambda_{\nu_{en}}(r) + \lambda_{\bar{\nu}_{ep}}(r)}. \quad (32)$$

As discussed above, in the presence of neutrino flavor/type transformation, the decrease of $\lambda_{\nu_{en}}$ due to conversion of ν_e into ν_μ or ν_τ in addition to the geometric decrease common to both $\lambda_{\nu_{en}}$ and $\lambda_{\bar{\nu}_{ep}}$ tends to lower Y_e^{EQ} at larger radius. Thus we have $dY_e^{\text{EQ}}/dr < 0$.

On the other hand, the Y_e evolution of a fluid element prior to the point of alpha-particle formation is governed by

$$v(r) \frac{dY_e(r)}{dr} = \lambda_{\nu_{en}}(r) - [\lambda_{\nu_{en}}(r) + \lambda_{\bar{\nu}_{ep}}(r)] Y_e(r), \quad (33)$$

where $v(r)$ is the outflow velocity at radius r . To first order, the solution to Eq. (33) is

$$Y_e(r) \approx Y_e^{\text{EQ}}(r) - \frac{v(r)}{\lambda_{\nu_{en}}(r) + \lambda_{\bar{\nu}_{ep}}(r)} \frac{dY_e^{\text{EQ}}(r)}{dr}. \quad (34)$$

As the fluid element moves to larger radius, the conversion ‘‘front’’ at E_ν^{RES} moves towards the high-energy end of the ν_e energy distribution function (shown schematically in Figure

3), causing Y_e^{EQ} to decrease. However, according to Eq. (34), this acts to increase Y_e above Y_e^{EQ} . Further, a larger increase is obtained for a larger outflow velocity v corresponding to a more rapid expansion of the fluid element. Consequently, flavor evolution of ν_e with energies important for determining Y_e can occur with $Y_e \gtrsim 1/3$ in the rapidly expanding neutrino-heated ejecta for a range of outflow conditions and neutrino mixing parameters.

As indicated in Eq. (31), the resonance energy E_ν^{RES} at a given radius depends on the effective neutrino numbers relative to baryons Y_{ν_e} , Y_{ν_μ} , and Y_{ν_τ} . These quantities determine the effects of the neutrino backgrounds on neutrino flavor/type evolution. Using Eq. (9) and assuming adiabatic neutrino evolution, we find that for a radially travelling neutrino,

$$Y_{\nu_e} \approx A_{\nu_e} \left[L_{\nu_e,50} \left(\frac{10 \text{ MeV}}{\langle E_{\nu_e} \rangle} \right) \int_{E_\nu^{\text{RES}}}^{\infty} f_{\nu_e}(E_{\nu_e}) dE_{\nu_e} - L_{\bar{\nu}_e,50} \left(\frac{10 \text{ MeV}}{\langle E_{\bar{\nu}_e} \rangle} \right) \right], \quad (35)$$

where

$$A_{\nu_e} = 0.723 \left(\frac{1.4 M_\odot}{M_{\text{NS}}} \right)^3 \frac{S_{100}^4 r_6^3}{R_{\nu,6}^2} \left[1 - \sqrt{1 - \frac{R_{\nu,6}^2}{r_6^2}} \right]^2, \quad (36)$$

and

$$f_{\nu_e}(E_{\nu_e}) = \frac{1}{T_{\nu_e}^3 F_2(\eta_{\nu_e})} \frac{E_{\nu_e}^2}{\exp(E_{\nu_e}/T_{\nu_e} - \eta_{\nu_e}) + 1} \quad (37)$$

is the normalized ν_e energy distribution function. In Eqs. (35) and (36) $L_{\nu_e,50}$ and $L_{\bar{\nu}_e,50}$ are the neutrino energy luminosities in units of 10^{50} ergs s^{-1} and $R_{\nu,6}$ is the neutrino-sphere radius in units of 10^6 cm. In Eq. (37) $F_2(\eta_{\nu_e}) \equiv \int_0^\infty x^2 / [\exp(x - \eta_{\nu_e}) + 1] dx$ is the second-order relativistic Fermi integral, and the two parameters T_{ν_e} and η_{ν_e} can be specified by fitting the first two energy moments of the numerical ν_e energy spectrum from supernova neutrino transport calculations. Expressions for Y_{ν_μ} and Y_{ν_τ} can be obtained in similar manner.

For $r \gtrsim 1.5R_\nu$, Eq. (36) can be rewritten as

$$A_{\nu_e} \approx 0.08 \left(\frac{T_9}{10} \right) \left(\frac{1.4 M_\odot}{M_{\text{NS}}} \right)^4 R_{\nu,6}^2 S_{100}^5. \quad (38)$$

Taking, for example, $L_{\nu_e} \sim L_{\bar{\nu}_e} \sim 10^{50}$ erg s^{-1} , $\langle E_{\nu_e} \rangle \approx 11$ MeV, and $\langle E_{\bar{\nu}_e} \rangle \approx 16$ MeV, which are plausibly characteristic of neutrino emission at very late times, we have $|Y_{\nu_e}| \sim 0.01$ at

$T_9 \sim 10$ for $R_{\nu,6} = 1$ and $S_{100} = 0.7$. Therefore, compared with typical values of $Y_e \sim 0.4$, Y_{ν_e} , Y_{ν_μ} , and Y_{ν_τ} can be neglected. Further, the effects of the neutrino backgrounds on neutrino flavor/type evolution are especially small for low values of S_{100} [see Eq. (38)]. This is because important neutrino flavor/type evolution occurs over a relatively narrow range of temperatures and for a lower entropy, these temperatures correspond to larger radii [see Eq. (1)] where neutrino fluxes are smaller.

In order to disable the alpha effect, we would like to have the bulk of the ν_e flux at $E_{\nu_e} < 20$ MeV (see Fig. 3) transformed away before the point of alpha-particle formation ($T_9 \sim 10$). This requires that the ν_e conversion front be at $E_\nu^{\text{RES}} \approx 20$ MeV when the neutrino-heated ejecta has reached the radius corresponding to $T_9 \approx 10$. With a typical entropy of $S_{100} = 0.7$ and values of $Y_e \sim 0.4 \gg Y_{\nu_e}, Y_{\nu_\mu}, Y_{\nu_\tau}$ in the ejecta, we see from Eq. (31) that this requirement is indeed fulfilled for $\delta m_{\mu^*e}^2 \approx 6$ eV².

The typical evolution of Y_e in the neutrino-heated ejecta with $\nu_\mu^* \rightleftharpoons \nu_s$ plus $\nu_\mu^* \rightleftharpoons \nu_e$ transformation can then be summarized as follows. At $T_9 \sim 20$, the electron fraction has a typical value of $Y_e \sim 0.4$ in equilibrium with the ν_e and $\bar{\nu}_e$ fluxes. As the ejecta moves to regions of lower temperature, the ν_e conversion front at E_ν^{RES} moves towards the high-energy end of the ν_e energy distribution function and removes the ν_e flux at $E_{\nu_e} < E_\nu^{\text{RES}}$. This suppresses the destruction of neutrons and lowers Y_e somewhat below ~ 0.4 . However, ν_e conversion coupled with the expansion of the ejecta causes rapid change in the instantaneous equilibrium Y_e value, Y_e^{EQ} , and maintains $Y_e > Y_e^{\text{EQ}}$. Consequently, conversion of ν_e with energies important for determining Y_e is completed at $Y_e > 1/3$. When the ejecta reaches the point of alpha-particle formation at $T_9 \sim 10$, the ν_e conversion front is at $E_\nu^{\text{RES}} \approx 20$ MeV and the bulk of the ν_e flux has been removed. This then defeats the alpha effect which would drive Y_e close to 0.5 if a significant flux of ν_e existed to destroy neutrons at $T_9 \lesssim 10$.

Therefore, our scenario of $\nu_\mu^* \rightleftharpoons \nu_s$ plus $\nu_\mu^* \rightleftharpoons \nu_e$ transformation ensures that $1/3 < Y_e \lesssim 0.4$ can be obtained and *maintained* before the onset of rapid neutron capture in the neutrino-heated ejecta. While this scenario does not lead to very low values of Y_e , it nevertheless guarantees a range of Y_e that will lead to a successful r -process when combined

with the appropriate entropy S and the dynamic expansion timescale τ_{DYN} in the ejecta.

V. CONCLUSIONS

The alpha effect is the single biggest impediment to obtaining the necessary conditions for r -process nucleosynthesis in neutrino-heated ejecta from supernovae. In fact, this effect may also be an obstacle for r -process nucleosynthesis in neutrino-heated ejecta from neutron-star mergers. The central problem is that the ν_e flux causing ejection of baryons from deep in the gravitational potential well of the neutron star will destroy neutrons via $\nu_e + n \rightarrow p + e^-$ in the regions of alpha-particle formation. This destruction of neutrons then renders the subsequent neutron capture process incapable of producing the heavy r -process elements. We have suggested a scheme of neutrino masses and mixings which could solve this conundrum by removing the ν_e flux through matter-enhanced $\nu_{\mu,\tau} \rightleftharpoons \nu_s$ plus $\nu_{\mu,\tau} \rightleftharpoons \nu_e$ transformation above the regions of efficient neutrino heating but below the regions of alpha-particle formation. This scheme which rescues r -process nucleosynthesis in neutrino-heated ejecta originally was not constructed for this purpose. Rather, it was designed to explain simultaneously the solar neutrino data and the anomalous atmospheric ν_μ/ν_e ratio and to allow for a hot component of dark matter. Subsequently, it also explained the LSND signal. In fact, this scheme with a maximally-mixed ν_μ - ν_τ doublet split from a lower-mass ν_e - ν_s doublet by $(\delta m^2)_{\text{LSND}} \gtrsim 1 \text{ eV}^2$ may be the only one which can escape elimination by recent interpretations of the SuperK atmospheric neutrino data [7,25] and by Big Bang Nucleosynthesis considerations [34].

While we do not know if there is a way other than invoking neutrino mixing to circumvent the alpha effect in neutrino-heated ejecta, attempts at “astrophysical” dodge of this effect made so far (see, e.g., Ref. [11]) seem to be finely tuned at best. Absent a non-neutrino-physics escape from the alpha effect, we could draw interesting inferences about Galactic chemical evolution were future experiments to reveal a neutrino mass scheme *other* than the one that aids the r -process. In that case, for example, we could be forced to re-think the origin of the bulk of the r -process material in the Galaxy. In turn, this could have

consequences for our understanding of the rates and physics of, e.g., neutron-star mergers. Or we could be forced to re-think electromagnetic ejection of material from supernovae.

In addition to the r -process connection, our scheme of neutrino masses and mixings has interesting consequences for detection of neutrinos from future Galactic supernovae. As the solar neutrino problem is solved by $\nu_e \rightleftharpoons \nu_s$ mixing in this scheme, sterile neutrinos produced by the $\nu_{\mu,\tau} \rightleftharpoons \nu_s$ transformation near the neutron star will be converted into ν_e . Therefore, at late times of the supernova process, there may be a significant *increase* in the average ν_e energy with no accompanying increase in the average $\bar{\nu}_e$ energy. Furthermore, it has been shown that neutrino flavor transformation has important effects on the dynamics of supernova explosion [29–32]. Conceivably, neutrino mixing also affects the nucleosynthesis discussed in Ref. [35], which occurs shortly after the supernova explosion. Currently, we are investigating the effects of our scheme of neutrino masses and mixings at these early times.

From this work, one conclusion specific to particle physics is that evasion of the alpha effect and, hence, robust production of the r -process elements in neutrino-heated ejecta seem to require at least one light sterile neutrino species. We have shown here that one neutrino mass scheme to disable the alpha effect has a maximally-mixed ν_μ - ν_τ doublet split from a lower-mass ν_e - ν_s doublet. However, another scheme [33], which has three light, nearly-degenerate active neutrinos and a heavier sterile neutrino species, has also been suggested to do the same. Though this latter scheme has the attractive feature of a significant increase in the neutron excess, considerations that do not concern the r -process argue against it. Finally, if we adopt the neutrino mass scheme of this paper, then the splitting between the doublets must be $\delta m^2 \gtrsim 1 \text{ eV}^2$ in order to have the beneficial effects on the r -process. Note that this splitting is within the LSND range and most likely in the upper sector of it. Of course, these conclusions presuppose that *some* of the r -process material in the Galaxy originated in neutrino-heated ejecta (from either supernovae or neutron-star mergers) and that there is no conventional astrophysical fix for the alpha effect.

Our conclusions will be tested by neutrino experiments as well as and astrophysical observations on r -process nucleosynthesis. In any case, it is both surprising and tantalizing

that mixings among active and sterile neutrino species with small masses can have such profound effects on the physics of astrophysical objects and the synthesis of the heaviest elements.

ACKNOWLEDGMENTS

We would like to acknowledge discussions with A. B. Balantekin, J. Fetter, G. C. McLaughlin, M. Patel, and J. R. Wilson. This work was partially supported by DOE Grant DE-FG03-91ER40618 at UCSB, by NSF Grant PHY98-00980 at UCSD, and by DOE Grant DE-FG02-87ER40328 at UMN.

REFERENCES

- [1] E. M. Burbidge, G. R. Burbidge, W. A. Fowler, and F. Hoyle, *Rev. Mod. Phys.* **29**, 624 (1957); A. G. W. Cameron, *PASP*, **69**, 201 (1957).
- [2] J. N. Bahcall, *Neutrino Astrophysics*, (Cambridge University Press, Cambridge 1989); for more recent discussions see W. C. Haxton, *Ann. Rev. Astron. Astrophys.* **33**, 459, (1995); J. N. Bahcall, *Astrophys. J.*, **467**, 475 (1996); Castellani *et al.* *Phys. Rep.*, **281**, 1 (1997).
- [3] T. K. Gaiser, F. Halzen, T. Stanev, *Phys. Rep.*, **258**, 173 (1995); Y. Fukuda *et al.*, *Phys. Lett.* **B433**, 9 (1998); *Phys. Lett.* **B436**, 33 (1998); and *Phys. Rev. Lett.* **81**, 1562 (1998).
- [4] C. Athanassopoulus *et al.* (LSND Collaboration), *Phys. Rev. Lett.* **75**, 2650 (1995); *Phys. Rev.* **C54**, 2685 (1996); *Phys. Rev. Lett.* **77**, 3082 (1996); *Phys. Rev. Lett.* **81**, 1774 (1998).
- [5] G. L. Fogli, E. Lisi, D. Montanino, and G. Scioscia, *Phys. Rev.* **D 56**, 4365 (1997); G. L. Fogli, E. Lisi, A. Marrone, and G. Scioscia, hep-ph/9906450; C. Y. Cardall and G. M. Fuller, *Phys. Rev.* **D 53**, 4421 (1996); A. Acker and S. Pakvasa, *Phys. Lett. B* **397**, 209 (1997); E. Ma and P. Roy, *Phys. Rev. Lett.* **80**, 4637 (1998); C. Y. Cardall, G. M. Fuller, and D. Cline, *Phys. Lett. B* **413**, 246 (1997).
- [6] D. O. Caldwell in “Perspectives in Neutrinos, Atomic Physics and Gravitation,” *Editions Frontieres*, ed. J. Tran Thanh Van *et al.*, (Gif-sur-Yvette, France, 1993); D. O. Caldwell and R. N. Mohapatra, *Phys. Rev.* **D 48**, 3259 (1993); *Phys. Lett B* **354**, 371 (1995); J. T. Peltoniemi and J. W. F. Valle, *Nucl. Phys. B* **406**, 409 (1993); G. M. Fuller, J. R. Primack, and Y.-Z. Qian, *Phys. Rev.* **D 52**, 1288 (1995).
- [7] V. Barger, S. Pakvasa, T. J. Weiler, and K. Whisnant *Phys. Rev.* **D58**, 093016 (1998).
- [8] Particle Data Group, *Eur. Phys. J.* **C3**, 319 (1998).

- [9] B. S. Meyer, W. M. Howard, G. J. Mathews, S. E. Woosley, R. D. Hoffman, *Astrophys. J.*, **399**, 656 (1992); S. E. Woosley, J. R. Wilson, G. J. Mathews, R. D. Hoffman, and B. S. Meyer, *Astrophys. J.*, **433** 299 (1994); K. Takahashi, J. Wittl, and H.-Th. Janka, *Astron. Astrophys.* **286**, 857 (1994).
- [10] R. D. Hoffman, S. E. Woosley, and Y.-Z. Qian, *Astrophys. J.*, **482**, 951 (1996); B. S. Meyer and J. S. Brown, *Astrophys. J. Suppl.*, **112**, 199 (1997).
- [11] Y.-Z. Qian and S. E. Woosley, *Astrophys. J.*, **471**, 331 (1996); G. M. Fuller and Y.-Z. Qian, *Nucl. Phys.* **A606**, 167 (1996); C. Y. Cardall and G. M. Fuller, *Astrophys. J.* **486**, L111 (1997); J. Samuelson and J. R. Wilson, *Astrophys. J.*, in press (1999).
- [12] G. C. McLaughlin and G. M. Fuller, *Astrophys. J.*, **472**, 440 (1996); The neutron deficit problem will obtain for any *neutrino-heated* ejecta. So to the extent that neutrinos supply the energy for material ejection and set Y_e in the ejecta, our nucleosynthesis considerations would also apply in the multi-dimensional scenarios of Ref. [16].
- [13] B. S. Meyer, G. C. McLaughlin, and G. M. Fuller, *Phys. Rev.* **C 58**, 3696 (1998).
- [14] W. C. Haxton, K. Langanke, Y.-Z. Qian, and P. Vogel, *Phys. Rev. Lett.*, **78**, 2694 (1997); Y.-Z. Qian, W. C. Haxton, K. Langanke, and P. Vogel, *Phys. Rev.* **C 55**, 1532 (1997).
- [15] C. Sneden, A. McWilliam, G. W. Preston, J. J. Cowan, D. L. Burris, and B. J. Armosky, *Astrophys. J.* **467**, 819 (1996); C. Sneden, J. J. Cowan, D. L. Burris, and J. W. Truran, *Astrophys. J.* **496**, 235 (1998); C. Sneden, S. Burles, G. M. Fuller, J. J. Cowan, T. Beers, and D. L. Burris, in preparation (1999).
- [16] D. S. Miller, J. R. Wilson, and R. W. Mayle, *Astrophys. J.*, **415**, 278 (1993); M. Herant, W. Benz, W. R. Hix, C. L. Fryer, and S. A. Colgate, *Astrophys. J.*, **435**, 339 (1994); A. Burrows, J. Hayes, and B. A. Fryxell, *Astrophys. J.*, **450**, 830 (1995); H.-T. Janka and E. Müller, *Astron. Astrophys.* **306**, 167 (1996); A. Mezzacappa, A. C. Calder, S.

- W. Bruenn, J. M. Blondin, M. W. Guidry, M. R. Strayer, and A. S. Umar, *Astrophys. J.* **495**, 911 (1998).
- [17] A. S. Burrows, presentation at ICAHTLT, Sedona, AZ, August 1999, and in preparation (1999).
- [18] Y.-Z. Qian, G. M. Fuller, G. J. Mathews, R. W. Mayle, J. R. Wilson and S. E. Woosley, *Phys. Rev. Lett.* **71**, 1965 (1993).
- [19] C. J. Horowitz and G. Li, *Phys. Rev. Lett.* **82**, 5198 (1999).
- [20] See, for example, A. Burrows and R. F. Sawyer, *Phys. Rev. C* **58**, 554 (1998) for effects of refined neutrino opacities in nuclear matter on neutrino emission in supernovae.
- [21] G. M. Fuller and B. S. Meyer, *Astrophys. J.*, **453**, 792 (1995).
- [22] J. N. Bahcall, P. Krastev, A. Yu. Smirnov, *Phys. Rev D* **58**, 096016 (1998).
- [23] G. C. McLaughlin and J. N. Ng, *Physics Letters B*, in press (1999), hep-ph/9907449.
- [24] J. R. Primack, J. Holtzman, A. Klypin, and D. O. Caldwell, *Phys. Rev. Lett.* **74**, 2160 (1995).
- [25] S. M. Bilenky, G. Giunti, and W. Grimus, *Eur. Phys. J.*, **C1**, 247 (1998).
- [26] X. Shi, D. N. Schramm, and B. Fields, *Phys. Rev. D* **48**, 2563 (1993). It should be noted, however, that the whole issue of the ^4He yield in BBN in the presence of matter-enhanced active-sterile neutrino transformations is controversial. See, e.g., X. Shi, *Phys. Rev. D* **54**, 2753 (1996); X. Shi and G. M. Fuller, *Phys. Rev. Lett.*, in press (1999); X. Shi, G. M. Fuller, and K. Abazajian, *Phys. Rev. D*, submitted (1999), astro-ph/9905259; R. Foot and D. Volkas, *Phys. Rev. D* **56**, 6653 (1997).
- [27] S. P. Mikheyev and A. Yu. Smirnov, *Sov. J. Nucl. Phys.* **24**, 913 (1985); L. Wolfenstein, *Phys. Rev. D* **17**, 2369 (1978).

- [28] J. T. Peltoniemi hep-ph/9511323 (unpublished) has suggested that this scheme of neutrino transformation could circumvent the r -process constraints of Ref. [18] on neutrino mixing, and could possibly lower Y_e . Along these lines, H. Nunokawa, J. T. Peltoniemi, A. Rossi, and J. Valle, Phys. Rev D **56**, 1704 (1997) suggested that $\nu_e \rightarrow \nu_s$ and $\bar{\nu}_e \rightarrow \bar{\nu}_s$ transformation would cause Y_e to reach the fixed point at $1/3$. However, this will not occur in a rapid outflow (see [33]). In any case, the simultaneous occurrence of $\nu_e \rightarrow \nu_s$ and $\bar{\nu}_e \rightarrow \bar{\nu}_s$ transformation envisioned by Nunokawa et al. could not circumvent the alpha effect discussed in the present work.
- [29] G. M. Fuller, R. W. Mayle, B. S. Meyer, and J. R. Wilson, Astrophys J. **389**, 517 (1992).
- [30] Y.-Z. Qian and G. M. Fuller, Phys. Rev. D, **49**, 1762 (1996).
- [31] A. Mezzacappa and S. W. Bruenn, in Proceedings of Future Directions of Supernova Research: Progenitors to Remnants, Memoirs of the Italian Astronomical Society, in press (1999); A. Mezzacappa and S. W. Bruenn, in Proceedings of the Second International Workshop on the Identification of Dark Matter, (World Scientific, Singapore), in press (1999).
- [32] Nunokawa, H., Qian, Y.-Z., and Fuller. G. M., Phys. Rev. D **55**, 3265 (1997), E. Akhmedov, Phys. Lett. B BAJ213, **64** (1988), E. Akhmedov, A. Lanza, S. T. Petcov, and D. W. Sciama, Phys Rev. **D 55**, 515 (1997), E. Akhmedov and Z. G. Berezhiani, Nucl. Phys. B **373**, 479, (1992).
- [33] G. C. McLaughlin, J. Fetter, A. B. Balantekin, and G. M. Fuller, Phys. Rev. C **39**, 2873 (1999).
- [34] X. Shi. G. M. Fuller, and K. Abazajian, Phys. Rev. **D**, submitted (1999).
- [35] R. D. Hoffman, S. E. Woosley, G. M. Fuller, and B. S. Meyer, Astrophys. J., **460**, 478 (1996).

FIGURES

FIG. 1. The neutrino mass scheme discussed in this paper. A doublet of (near)-maximally-mixed ν_μ and ν_τ neutrinos with mass-squared difference $\delta m_{\mu\tau}^2 \sim 10^{-2} \text{ eV}^2$ is split from a doublet of lower-mass ν_e and ν_s by a mass-squared difference $\delta m_{\text{doublets}}^2$.

The lower-mass doublet can be arranged (lower right) with maximal (or near maximal) $\nu_e \rightleftharpoons \nu_s$ vacuum mixing to give a “just so” solar neutrino solution, which would require $\delta m_{e_s}^2 \sim 10^{-10} \text{ eV}^2$. Alternatively (lower left), the sterile neutrino could be heavier than the ν_e with $\delta m_{e_s}^2 \lesssim 10^{-5} \text{ eV}^2$ to give a matter-enhanced (MSW) solution to the solar neutrino problem. We assume that $\delta m_{\text{doublets}}^2$ is much larger than the mass-squared splittings within the doublets.

FIG. 2. Cartoon of the instantaneous neutrino mass levels (effective mass-squared m_{eff}^2) as functions of matter density ρ for $Y_e > 1/3$.


FIG. 3. Example ν_e and $\nu_{\mu,\tau}$ energy distribution functions. Here we take these functions to be of the form in Eq. (37) with $T_{\nu_e} = 2.75 \text{ MeV}$, $\eta_{\nu_e} = 3$ (corresponding to $\langle E_{\nu_e} \rangle = 11 \text{ MeV}$) and $T_{\nu_{\mu,\tau}} = 6.76 \text{ MeV}$, $\eta_{\nu_{\mu,\tau}} = 3$ (corresponding to $\langle E_{\nu_{\mu,\tau}} \rangle = 27 \text{ MeV}$). The resonance energy E_ν^{RES} for neutrino flavor/type transformation sweeps from low to high energy through the neutrino energy distribution functions as a fluid element moves away from the neutron star.

TABLES



TABLE I. Weak potentials derived from neutrino forward scattering on electron/nucleon (A) and neutrino (B) backgrounds for various channels of neutrino transformation. The corresponding antineutrino transformation channels have opposite signs for A and B . Here N_A is Avogadro's number, G_F is the Fermi constant, ρ is the matter density, Y_e is the electron fraction, and Y_{ν_e} , Y_{ν_μ} , and Y_{ν_τ} are the effective neutrino numbers for the corresponding species relative to baryons.



Channel	A	B
$\nu_e \rightleftharpoons \nu_s$	$(3\sqrt{2}/2)G_F\rho N_A (Y_e - 1/3)$	$\sqrt{2}G_F\rho N_A (2Y_{\nu_e} + Y_{\nu_\mu} + Y_{\nu_\tau})$
$\nu_\mu \rightleftharpoons \nu_s$	$(\sqrt{2}/2)G_F\rho N_A (Y_e - 1)$	$\sqrt{2}G_F\rho N_A (Y_{\nu_e} + 2Y_{\nu_\mu} + Y_{\nu_\tau})$
$\nu_\tau \rightleftharpoons \nu_s$	$(\sqrt{2}/2)G_F\rho N_A (Y_e - 1)$	$\sqrt{2}G_F\rho N_A (Y_{\nu_e} + Y_{\nu_\mu} + 2Y_{\nu_\tau})$
$\nu_\mu \rightleftharpoons \nu_e$	$\sqrt{2}G_F\rho N_A Y_e$	$\sqrt{2}G_F\rho N_A (Y_{\nu_e} - Y_{\nu_\mu})$
$\nu_\tau \rightleftharpoons \nu_e$	$\sqrt{2}G_F\rho N_A Y_e$	$\sqrt{2}G_F\rho N_A (Y_{\nu_e} - Y_{\nu_\tau})$
$\nu_\mu \rightleftharpoons \nu_\tau$	0	$\sqrt{2}G_F\rho N_A (Y_{\nu_\mu} - Y_{\nu_\tau})$

$$\delta m_{\mu-\tau}^2 \sim 10^{-2} \text{ eV}^2$$

ν_μ  ν_τ

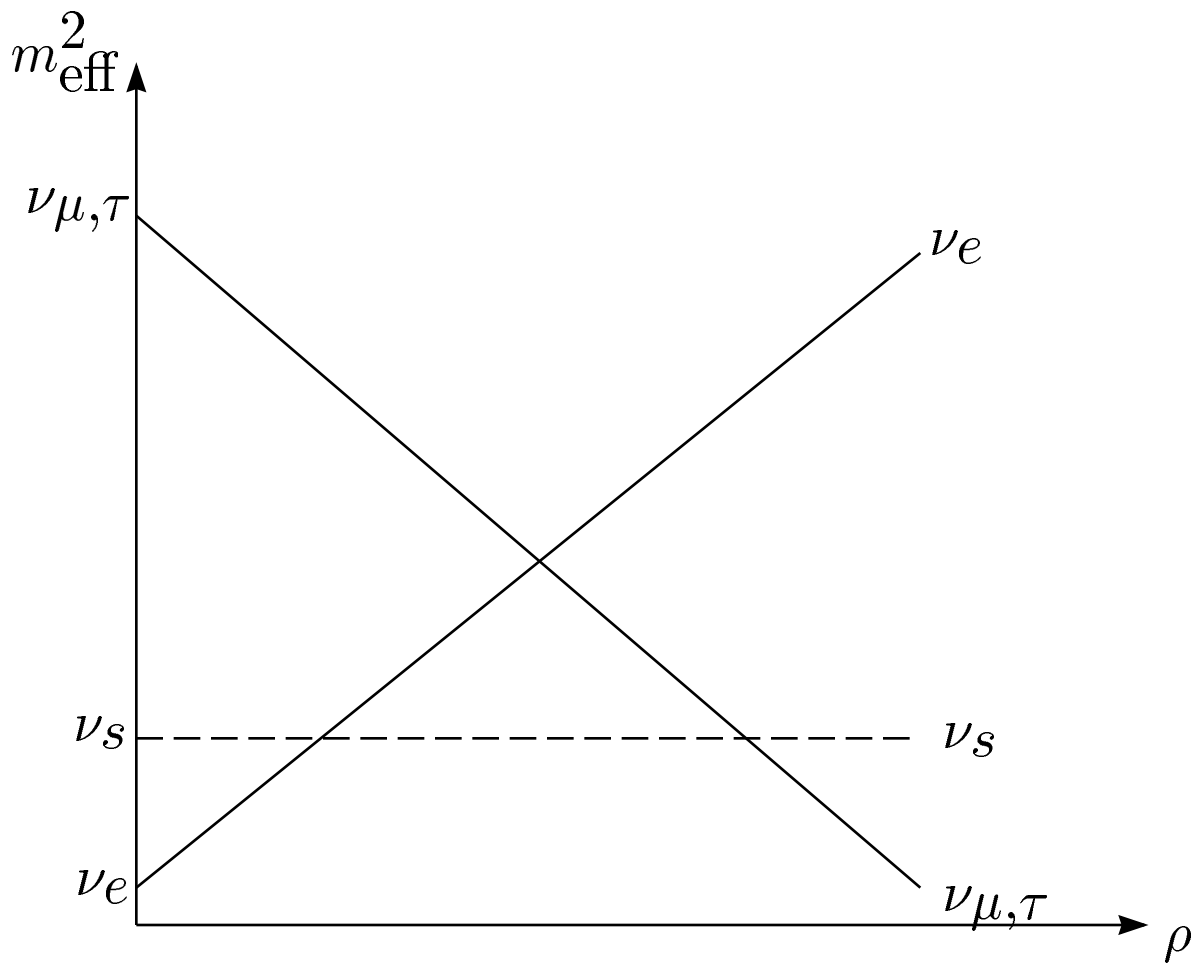
$\delta m_{\text{doublets}}^2$

ν_s 
 ν_e 

ν_s 
 ν_e 

$$\delta m_{se}^2 \leq 10^{-5} \text{ eV}^2$$

$$\delta m_{e-s}^2 \sim 10^{-10} \text{ eV}^2$$



Fast expansion case: $\nu_{\mu,\tau} \rightleftharpoons \nu_s$
followed by $\nu_{\mu,\tau} \rightleftharpoons \nu_e$

In the fast expansion case, Y_e lags neutrino transformation. Therefore, the order of the level crossings does not change until all of the electron neutrinos are transformed.

Net Result: Probability $\nu_\mu \rightarrow \nu_\mu \Rightarrow 1/4$
 Probability $\nu_\mu \rightarrow \nu_\tau \Rightarrow 1/4$
 Probability $\nu_\mu \rightarrow \nu_s \Rightarrow 1/2$
 Probability $\nu_{\mu,\tau} \rightarrow \nu_e \Rightarrow 0$ (2nd resonance)

